GCB Bioenergy

WILEY

Global Change Biology Bioenergy
BIOPRODUCTS FOR A SUSTAINABLE BIOECONOMY

RESEARCH ARTICLE OPEN ACCESS

Genetic Basis of Non-Photochemical Quenching and Photosystem II Efficiency Responses to Chilling in the Biomass Crop *Miscanthus*

Asha Kumari[1] | Joyce N. Njuguna[2] | Xuying Zheng[2,3] | Johannes Kromdijk[4] | Erik J. Sacks[2,3] | Katarzyna Glowacka[1,5]

[1]Department of Biochemistry and Center for Plant Science Innovation, University of Nebraska-Lincoln, Lincoln, Nebraska, USA | [2]Department of Crop Sciences, University of Illinois, Urbana, Illinois, USA | [3]DOE Center for Advanced Bioenergy and Bioproducts Innovation, University of Illinois, Urbana, Illinois, USA | [4]Department of Plant Science, University of Cambridge, Cambridge, UK | [5]Institute of Plant Genetics, Polish Academy of Sciences, Poznań, Poland

Correspondence: Katarzyna Glowacka (kglowacka2@unl.edu)

Received: 26 August 2024 | **Revised:** 26 November 2024 | **Accepted:** 2 December 2024

Funding: This work was supported by the National Science Foundation under IOS-2142993 (CAREER) award to KG, by the DOE Office of Science, Office of Biological and Environmental Research (BER) grant no. DE-SC0012379 to ES and by the DOE Center for Advanced Bioenergy and Bioproducts Innovation (U.S. Department of Energy, Office of Science, Biological and Environmental Research Program under Award Number DE-SC0018420) to ES. Any opinions, findings, conclusions or recommendations expressed in this publication are those of the author(s) and do not necessarily reflect the views of the U.S. Department of Energy.

Keywords: chilling tolerance | genome-wide association study | kinetics of photosynthetic processes | *Miscanthus sacchariflorus* | natural genetic variation | non-photochemical quenching | photosynthesis | photosystem II efficiency

ABSTRACT

Miscanthus holds a promise as a biocrop due to its high yield, perenniality and ability to grow on infertile soils. However, the current commercial biomass production of *Miscanthus* is mostly limited to a single sterile triploid clone of *M.* × *giganteus*. Nevertheless, parental species of *M.* × *giganteus, Miscanthus sacchariflorus* and *Miscanthus sinensis* contain vast genetic diversity for crop improvement. With *M. sacchariflorus* having a natural geographic distribution in cold-temperate northeast China and eastern Russia, we hypothesised that it has substantial variation in physiological response to chilling. Using a semi-high-throughput method, we phenotyped 209 *M. sacchariflorus* genotypes belonging to six genetic groups for non-photochemical quenching (NPQ) and photosystem II efficiency (ΦPSII) kinetics under warm and chilling treatments in three growing seasons. In response to the chilling treatment, all genetic groups exhibited an increase in NPQ induction rate indicating faster activation of NPQ in light. Notably, under chilling, the Korea/NE China/Russia 2x and N China 2x groups stood out for the highest NPQ rate in light and the highest steady-state NPQ in light. This NPQ phenotype may contribute adaptation to chilling during bright, cold mornings of spring and early autumn in temperate climates, when faster NPQ would better protect from oxidative stress. Such enhanced adaptation could expand the growing season and thus productivity at a given location or expand the range of economically viable growing locations to higher latitudes and altitudes. A genome-wide association study identified 126 unique SNPs associated with NPQ and ΦPSII traits. Among the identified candidate genes were enzymes involved in the ascorbate recycle and shikimate pathway, gamma-aminobutyric acid and cation efflux transporters. Identifying natural variation and genes involved in NPQ and ΦPSII kinetics considerably enlarges the toolbox for breeding and/or engineering *Miscanthus* with optimised photosynthesis under warm and chilling conditions for sustainable feedstock production for bioenergy.

Asha Kumari and Joyce N. Njuguna contributed equally to this work.

Chilling affects the productivity and geographical distribution of most crops. Using a semi-high-throughput approach to investigate photosynthesis-related traits, we characterised variation existing in the bioenergy crop *Miscanthus* under chilling and warm conditions and identified potential genes associated with it. Under chilling, two genetic groups from the northern edge of *Miscanthus* distribution stood out for faster activation of photoprotection. This trait may contribute adaptation to chilling in temperate climates, when faster photoprotection would better defend from oxidative stress. Enhanced chilling adaptation could expand the growing season and thus productivity or enlarge the range of growing locations.

1 | Introduction

Miscanthus is a fast-growing C_4 grass and an emerging biomass crop for biofuel and bioproducts (Clifton-Brown, Harfouche et al. 2019; Lee et al. 2018; Somerville et al. 2010). As a perennial rhizomatous plant with high nutrient-use efficiency, *Miscanthus* can grow on soils of low fertility and with low agronomic inputs (Clifton-Brown, Schwarz et al. 2019; Mitros et al. 2020). However, currently a single sterile triploid clone of *Miscanthus* × *giganteus*, referred to as '1993–1780' or 'Illinois' (Głowacka et al. 2015; Hodkinson and Renvoize 2001), is primarily grown commercially for biomass production. Reliance on a single clone is a great risk for pest and disease outbreaks. Though *M.* × *giganteus* '1993–1780' has high chilling tolerance (Friesen et al. 2014; Głowacka et al. 2014; Naidu et al. 2003; Wang et al. 2008), its winter hardiness is insufficient in USDA hardiness zone 5b (average annual minimum temperature of −26.1 to −23.3°C) or lower.

The parental species of *M.* × *giganteus* are *Miscanthus sacchariflorus* and *Miscanthus sinensis*, which contain vast genetic diversity for improving *Miscanthus* as a biocrop (Clark et al. 2019; Sacks et al. 2013). Of these two species, *M. sacchariflorus* has the most northern geographical distribution, from ~50° N along the eastern portion of the Amur River watershed in eastern Russia, through the Korean peninsula, Japan and northeastern China to ~28° N along the Yangtze River watershed, including hardiness zones 3–8 (−40 to −12.2°C average annual minimum air temperature) (Clark et al. 2019; Clifton-Brown, Chiang, and Hodkinson 2008). In contrast, most C_4 grasses, including those most closely related to *Miscanthus*, such as *Saccharum*, *Sorghum* and *Zea*, have a natural geographic range limited entirely or primarily to the tropics and subtropics and did not evolve photosynthetic adaptation to chilling. Notably, under cold temperatures (10°C–16°C), some *Miscanthus* accessions maintain a substantial proportion of photosynthetic capacity (Naidu et al. 2003; Friesen et al. 2014). For instance, *M.* × *giganteus* maintains about 50% of its maximum carbon assimilation capacity at 4°C, which is significantly higher than many other C_4 plants. Consistent with its extreme northern geographical distribution, some *M. sacchariflorus* from eastern Russia have been shown to be a source of exceptional chilling-tolerant C_4 photosynthesis (Pignon et al. 2019) and winter hardiness (Dong et al. 2019). Thus, we hypothesised that substantial variation in physiological response to chilling, especially related to photosynthesis, exists within *M. sacchariflorus*.

Chilling is among the foremost abiotic stresses affecting the productivity and geographical distribution of most crops (Chiluwal et al. 2018; Langholtz, Stokes, and Eaton 2016; Ma et al. 2015). Low temperature adversely affects photosynthesis by reducing the rate of enzymatic reactions in the Calvin–Benson cycle, limiting the sinks for the absorbed excitation energy (light) and leading to the formation of reactive oxygen species (ROS) and subsequent photodamage. The excess of energy can be harmlessly released as heat, which can be measured as non-photochemical quenching (NPQ) of chlorophyll fluorescence (Müller, Li, and Niyogi 2001). Therefore, NPQ plays an important role in defense against abiotic stresses (Brüggemann et al. 2009; Malnoë 2018). However, NPQ impairment causes higher ROS production (Roach and Krieger-Liszkay 2012), whereas resistance to photoinhibition in chilling has often been identified as a trait closely related to chilling tolerance (Rapacz et al. 2008). There have also been examples of species that under extreme abiotic stress maintain a high-sustained NPQ to avoid photo-oxidative damage (Adams and Demmig-Adams 1994; Brüggemann et al. 2009; Fernández-Marín et al. 2018; Savitch et al. 2002). NPQ involves the xanthophyll cycle, composed of violaxanthin (*V*), intermediate antheraxanthin (*A*) and zeaxanthin (*Z*). The xanthophyll cycle is operated by de-epoxidation of *V* to *A* and then to *Z* via the enzyme violaxanthin de-epoxidase (VDE), where Z is assumed to be energy quencher (Demmig-Adams 1990; Yamamoto, Nakayama, and Chichester 1962). In low light-limited conditions, *Z* can be converted back to *V* by the enzyme zeaxanthin epoxidase (ZEP). Another component of NPQ is the build up of a proton gradient across the thylakoid membrane causing protonation of photosystem II subunit S (PsbS) triggering conformational changes in antenna complexes necessary for heat release (Li et al. 2000). The major and fastest NPQ component is energy-dependent quenching, qE, which molecularly depends on PsbS, VDE and ZEP, whereas zeaxanthin-dependent quenching, qZ, works independently from PsbS and proton gradient across the thylakoid membrane involving a conformational change of at least the minor antennas (Dall'Osto, Caffarri, and Bassi 2005; Nilkens et al. 2010). Here, we investigated NPQ timepoints that largely belonged to qE and qZ by measuring NPQ in 10 min in high light followed by 12 min of dark. Although light exposure allows one to estimate the induction rate of NPQ and its maximum level, the 12 min in the dark allows us to estimate the rate of NPQ relaxation and its residual values (Sahay et al. 2023). Simultaneously with NPQ, the kinetics of operating efficiency of photosystem II (ΦPSII) was estimated. ΦPSII has been shown to be tightly linked to the quantum yield of CO_2 fixation (ΦCO_2) measured by gas exchange in C_4 species (Leipner, Fracheboud, and Stamp 1999; Cousins et al. 2002). As NPQ and PSII can compete for energy under fluctuating light conditions, it has been shown that NPQ can transiently limit ΦCO_2 (Kromdijk et al. 2016).

This study was conducted to (1) quantify variation in response of photosynthesis-related traits to chilling in a *M. sacchariflorus* diversity panel consisting of 209 accessions in six genetic

groups (Clark et al. 2019) that had previously revealed great variation in biomass yield and yield component traits (Njuguna, Clark, Anzoua et al. 2023; Njuguna, Clark, Lipka et al. 2023), (2) elucidate the physiological mechanisms of chilling-tolerant photosynthesis in this species and (3) identify genomic regions and candidate genes that confer chilling-tolerant physiology. Traditional plant physiological analysis methods are often time-consuming and far from being high throughput. Thus, we investigated NPQ and ΦPSII from leaf disks collected in 96-well plates and then dark-adapted overnight to minimise the effect of microenvironmental conditions at the time of sampling (i.e., light intensity, temperature and time of day) (Sahay et al. 2023). We quantified, under warm and chilling treatments, variation in the kinetics of NPQ as an estimate of photoprotection and variation in the operating quantum yield of photosystem II (ΦPSII) as an estimate of the efficiency of the light reaction of photosynthesis to understand the response of *M. sacchariflorus* to chilling stress. We identified *M. sacchariflorus* genetic groups that in response to chilling upregulated the speed of NPQ induction, which can play an important role in protection from oxidative stress during bright, chilling mornings of spring and early autumn in temperate climates. Additionally, we conducted genome-wide association studies (GWAS) to identify genomic regions and candidate genes associated with the regulation of NPQ and ΦPSII under warm and chilling conditions. Thus, the long-term goal of this work was to begin to establish an evidence-based path for breeding and/or engineering *Miscanthus* and other Saccharinae crops to have optimised photosynthesis for adaptation to chilling, a stress that occurs frequently at temperate latitudes early and late in the growing season. Such enhanced adaptation could expand the growing season and thus productivity at a given location or expand the range of economically viable growing locations to higher latitudes and altitudes. Both of these benefits would be expected to enhance climate resilience and given that the Saccharinae includes some of humanity's most important crops (e.g., maize, sugarcane and sorghum), they would be expected to improve agricultural productivity.

2 | Materials and Methods

2.1 | Plant Materials and Field Trials

Variation for photosynthetic-related traits in a *M. sacchariflorus* diversity panel was evaluated under warm and chilling treatments on field-grown plants. In total 209 *Miscanthus* genotypes were studied, including 205 *M. sacchariflorus* and four *M.* × *giganteus* genotypes [Dataset_1 (Kumari et al. 2024)]. The *M. sacchariflorus* genotypes were composed of 149 diploid and 56 tetraploid genotypes and belong to six genetic groups identified by Clark et al. (2019): N Japan 4x ($n = 4$), S Japan 4x ($n = 48$), N China/Korea/Russia 4x ($n = 4$), Korea/NE China/Russia 2x ($n = 144$), N China 2x ($n = 4$) and Yangtze 2x (ssp. *lutarioriparius*) ($n = 1$). The *M. sacchariflorus* genotypes were collected from the wild across East Asia (Table S1). Out of the four *M.* × *giganteus* genotypes, two were tetraploids and two triploids. *M.* × *giganteus* 3x '1993–1780' (UI10-00107, syn. 'Illinois') is the predominant commercial biomass cultivar of *Miscanthus* in North America and Europe because it is high yielding, broadly adapted and was first imported from Japan to Denmark in the mid-1930s (Głowacka et al. 2015; Kalinina et al. 2017; Linde-Laursen 1993). *M.* × *giganteus* '1993–1780' was used as a control for comparing variation in *M. sacchariflorus* because its high chilling tolerance of photosynthesis has been well documented (Friesen et al. 2014; Głowacka et al. 2014; Naidu et al. 2003; D. Wang et al. 2008). *M.* × *giganteus* 3x 'Nagara' (UI10-00123) is a recently introduced, high-yielding cultivar bred by M. Deuter (Tinplant, Klein Wanzleben, Germany; U.S. Plant Patent No.: USPP22,033P2) (Deuter, 2009) that is available commercially in the United States (https://aggrowtech.com/biomass-crops/). Ramets of the genotypes were established in a temperate environment field trial at the Energy Farm of the University of Illinois (UIUC) located 40.067 N, 88.198 W with an elevation of 223 m. The field was established on April 29–30, 2015 on drummer silty clay loam soil. The field plots were established in a randomised complete block design with four blocks of single-plant plots spaced 2.0 × 2.0 m in a grid of 15 × 15 (Table S1). Each block was surrounded by a border of *M.* × *giganteus* '1993–1780'. The four blocks were arranged in a 2 × 2 square. The field was fertilised with nitrogen fertiliser (80 kg ha^{-1}) each spring. When needed, weeds were controlled by mechanical methods and/or with herbicides. Climate data were recorded by a weather station on the UIUC Energy Farm (Figure S1).

2.2 | Collection of NPQ and ΦPSII Kinetics Data

In total, 25 NPQ and ΦPSII traits were studied (Table 1). NPQ and ΦPSII kinetics were delivered from leaf discs collected in the afternoon from the plots in the field trial during the summer of 2017, 2019 and 2020. The sample was during the field trial's third, fifth and sixth growth season from plants that were healthy and which had not passed their peak yield yet. NPQ and ΦPSII kinetics were investigated as previously described by Sahay et al. (2023) with minor modifications. Leaf discs of size 0.32 cm^2 were collected from the middle portion of the youngest fully expanded leaf, avoiding the midrib using a hole puncher, placed in a 96-well plate (167,008; Thermo Scientific) with their adaxial surface down followed by covering each disc with a moist sponge to prevent drying. Sponge cubes (approximately 1 × 1 × 0.5 cm) were cut from commercially available sponges and well rinsed. The plates with leaf material were wrapped in aluminum foil, placed upside down and then incubated in the dark overnight (~16 h) at room temperature of 20°C (warm) or 4°C (chilling). The following day, the discs in the plates were phenotyped at room temperature using a chlorophyll fluorescence imager (CF Imager, Technologica, Colchester, UK). There was no visible effect of keeping the leaf disk overnight at 4°C. Plates that received the chilling treatment were placed at room temperature in the dark for 20 min prior to imaging to prevent condensation in the bottom of the wells. Initially, the minimum (F_o) and maximal (F_m) fluorescence were measured in dark, followed by subsequent exposure of the leaf discs to light (2000 μmol m^{-2} s^{-1}) for 10 min followed by the dark for 12 min. Saturating flashes of 6000 μmol m^{-2} s^{-1} (provided by light $\lambda_{max} = 470$ nm) were used for capturing changes in maximum (F_m') and steady-state fluorescence (F_s) over the time in periods of light and dark. The saturating flashes were provided at intervals of 0, 0.33, 0.67, 1, 2, 3, 4, 5, 6, 7, 8, 9, 10, 10.33, 10.67, 11, 12, 13, 16, 19 and 22 min after beginning light exposure.

TABLE 1 | Description of non-photochemical quenching (NPQ) and photosystem II operating efficiency (ΦPSII) traits investigated in the present study.

Kinetics type	Trait	Mathematical description	Kinetics attribute	Biological description
NPQ induction in light	$NPQslope_{lightH}$	Initial slope of NPQ induction under high light estimated from hyperbolic (H) curve fit to NPQ	Rate	How fast NPQ is induced under light conditions resulting in plant photoprotection from excess light that prevents the likelihood of formation of damaging free radicals
	$NPQrate\_constant_{light}$	Rate in which NPQ reaches 63.2% of final steady-state value (min^{-1}) Calculated from exponential function (E)		
	$NPQslope_{lightL}$	Slope of linear function (L) fitted to the 0 and two first points of NPQ at light		
	$NPQasymptote_{lightH}$	The potential value for maximum NPQ under prolonged high light calculated from hyperbolic curve fit to NPQ	Steady state and range	The level and magnitude of NPQ response to the light conditions resulting in plant photoprotection from excess light that prevents the likelihood of formation of damaging free radicals
	$NPQasymptote_{lightE}$	Asymptote of exponential function (E) fit to NPQ		
	NPQ_{max}	The highest value of NPQ during induction		
NPQ relaxation in dark	$NPQrate\_constant_{dark}$	Rate in which NPQ reaches 63.2% of final steady-state value (min^{-1}) calculated from exponential function (E) fit to NPQ	Rate	How fast the NPQ relaxes under dark resulting in plant be able to funnel more energy to dive photosynthesis
	$NPQslope_{darkL}$	Slope of linear function (L) fitted to last point in light and two first points in dark of NPQ		
	$NPQslope_{darkH}$	Rate of NPQ relaxation after turning off lights estimated from a hyperbolic curve fit to NPQ		
	$NPQstart_{darkH}$	NPQ at the beginning of the dark treatments estimated from a hyperbolic curve fit to NPQ	Contribute to range	The magnitude of NPQ response in dark resulting in plant flexibility to adjust NPQ to the changeable light conditions
	$NPQamplitude_{darkE}$	Amplitude calculated from exponential function (E) fit to NPQ		
	$NPQamplitude_{darkH}$	Amplitude calculated from hyperbolic (H) curve fit to NPQ		
	NPQ_{end}	NPQ in the last point in dark (point 20th of assay)	Steady state	The remaining NPQ in dark resulting in plant prolonged photoprotection, usually higher in stress conditions like chilling
	$NPQresidual_{dark}$	Not relaxed NPQ at end of assay calculated from exponential function (E) fit to NPQ		

(Continues)

TABLE 1 | (Continued)

Kinetics type	Trait	Mathematical description	Kinetics attribute	Biological description
ΦPSII induction in dark	$\Phi PSIIslope_{darkH}$	Rate of ΦPSII induction in dark estimated from hyperbolic (H) curve fit to ΦPSII	Rate	How fast ΦPSII recovers following the light being switched off
	$\Phi PSIIrate\_constant_{dark}$	Rate in which ΦPSII reaches 63.2% of final steady state value in dark (min^{-1}) calculated from exponential equation (E) fit to ΦPSII		
	$\Phi PSII_{startH}$	ΦPSII in beginning of dark calculated from hyperbola (H) fit to ΦPSII	Contribute to range	The magnitude of ΦPSII response in dark resulting in plant flexibility to adjust ΦPSII to the changeable light conditions
	$\Phi PSII_{startE}$	ΦPSII at the beginning of the dark calculated from exponential function (E)		
	$\Phi PSIIamplitude_{darkH}$	Amplitude of hyperbola (H) fit to ΦPSII	Steady state and/or range and/or contribute to range	
	$\Phi PSIIamplitude_{darkE}$	Amplitude of exponential equation (E) fit to ΦPSII		
	$\Phi PSII_{start}$	ΦPSII in the first point measured in light		
	$\Phi PSII_{end}$	ΦPSIIin the last point of dark (point 20th of assay)		
	$\Phi PSII_{end}/\Phi PSII_{start}$	Ratio between ΦPSII in the last and first points of dark		
	$\Phi PSII_{end}/NPQ_{end}$	Ratio between ΦPSII and NPQ at the end of dark (point 20th of the assay)	N/A	Estimation of tradeoff between the quantum efficiency of photochemistry and photoprotection; higher ratio indicates more efficient recovery of ΦPSII in the end of dark period
	F_v/F_m	Maximum quantum yield of PSII measured before switching on light preceded by prolonged darkness		Trait correlated to the maximum quantum yield of photosynthesis because the existence of any type of stress would result in damage of PSII or the induction of sustained quenching; F_v/F_m is the most commonly used trait for measuring stress in leaves

NPQ was calculated using Equation (1), assuming the Stern–Volmer quenching model:

$$\mathrm{NPQ} = F_\mathrm{m}/F_\mathrm{m}' - 1 \quad (1)$$

Maximum and operating PSII efficiency was estimated from the fluorescence measurements according to Equations (2) and (3), respectively.

$$F_\mathrm{v}/F_\mathrm{m} = \left(F_\mathrm{m} - F_\mathrm{o}\right)/F_\mathrm{m} \quad (2)$$

$$\Phi\mathrm{PSII} = \left(F_\mathrm{m}' - F_\mathrm{s}\right)/F_\mathrm{m}' \quad (3)$$

The NPQ and ΦPSII data (Dataset S1) were fit to hyperbolic, exponential and linear equations 4–9 in MATLAB (Matlab R2019b; MathWorks, Natick, MA, USA) (Sahay et al. 2023).

$$\mathrm{NPQ} = \frac{time \times NPQslope_{lightH} + NPQasympotote_{lightH} - \sqrt{\begin{array}{l}\left(time \times NPQslope_{lightH} + NPQasymptote_{lightH}\right)^2 - \\ 4 \times 0.5 \times time \times NPQslope_{lightH} \times NPQasymptote_{lightH}\end{array}}}{(2 \times 0.5)} \quad (4)$$

$$\mathrm{NPQ} = NPQasympotote_{lightE} \times \left(1 - \exp^{\left(-NPQrate\_constant_{light} \times time\right)}\right) \quad (5)$$

$$\mathrm{NPQ} = NPQstart_{darkH} - \left(\frac{\begin{array}{c}\mathrm{time} \times \mathrm{NPQslope}_{dark\ H} + \mathrm{NPQamplitude}_{darkH} - \\ \sqrt{\left(time \times NPQslope_{darkH} + NPQamplitude_{darkH}\right)^2 - 4 \times 0.5 \times time \times NPQslope_{darkH} \times NPQamplitute_{darkH}}\end{array}}{(2 \times 0.5)}\right) \quad (6)$$

$$\mathrm{NPQ} = NPQamplitude_{darkE} \times \left(exp^{\left(-NPQrate\_constant_{dark} \times time\right)}\right) + NPQresidual_{dark} \quad (7)$$

$$\Phi\mathrm{PSII} = \Phi PSIIstart_{darkH} + \left(\frac{\begin{array}{c}\mathrm{time} \times \Phi\mathrm{PSIIslope}_{darkH} + \Phi\mathrm{PSIIamplitude}_{darkH} - \\ \sqrt{\left(time \times \Phi PSIIslope_{darkH} + \Phi PSIIamplitude_{darkH}\right)^2 - 4 \times 0.5 \times time \times \Phi PSIIslope_{darkH} \times \Phi PSIIamplitude_{darkH}}\end{array}}{(2 \times 0.5)}\right) \quad (8)$$

$$\Phi\mathrm{PSII} = \Phi PSIIamplitude_{darkE} \times \left(1 - exp^{\left(-\Phi PSIIrate\_constant_{dark} \times time\right)}\right) + \Phi PSII_{startE} \quad (9)$$

In total, 25 traits attributed to rate, amplitude and steady-state of kinetics were analyzed (Table 1). Goodness-of-fit tests were performed to assess the discrepancy between measured values and the values expected under the fit equations. Leaf discs from the warm control treatment having F_v/F_m values less than 0.55 were filtered out of the dataset and the rest were used for subsequent analysis. No such filter was applied to the chilling-treated discs. Additionally, for warm and chilling treatments, leaf discs having a goodness-of-fit value of fitting equations to NPQ and ΦPSII kinetics lower than 10 percentile were filtered out. In the growing season 2017, 2019 and 2020, a total of 1664, 1664 and 1672 leaf discs were collected, respectively, out of which half were incubated at 20°C overnight (warm treatment) and the other half were incubated at 4°C (chilling treatment). Of the collected discs in 2017, 2019 and 2020, 1073, 1082 and 1164, respectively, passed quality control and were used for downstream analyses of NPQ and ΦPSII traits. Because 2020 had the most complete set of data after quality control, which could be attributed to it being the wettest year compared to other 2 years, we describe here in more detail NPQ and ΦPSII variation between genetic groups in that year and compare it to other growing seasons for the trend in the chilling response of *M. sacchariflorus*.

2.3 | Statistical Analyses of Phenotyping Data

Correlation tests were performed between NPQ and ΦPSII traits using Pearson's correlation tests with corrpackage and the correlation matrix was visualised with corrplot in R (v 4.4.2). For each trait, an appropriate transformation to normalise the data was obtained with the Box-Cox procedure implemented in the R package MASS (Kafadar et al. 2002). Using transformed data, two types of analyses of variance (ANOVAs) were conducted, with fixed and completely random models. A linear model was fit for each of the traits (Equation 4), with μ as the grand mean, blocks (B) and genotype (G) as fixed effects, and ε as the standard error to estimate least square means (LS means) of traits for each genotype using the R package lsmeans (Lenth 2016). A completely random effects model ANOVA was fit for each of the traits (Equation 4), with blocks (B) and genotype (G) as random effects using the R package lme4 (Bates et al. 2015) to estimate variance components, which were subsequently used to estimate genotypic repeatabilities and best linear unbiased predictors (BLUPs). BLUPs were used as input for GWAS.

$$Y_{ij} = \mu + G_i + B_j + \varepsilon_{ij} \quad (10)$$

The extent to which phenotypic variation was accounted for by difference among clonal replicates of the genotypes was estimated as the repeatability (R) (Equation 11), where σ_G^2 and σ_ϵ^2 are the variance components estimated for the genotype and the residual, respectively, and n_B is the total number of replications. Variance components from the random effects model in Equation 10 were used to estimate repeatabilities for the 25 NPQ and ΦPSII traits.

$$R = \frac{\sigma_G^2}{\sigma_G^2 + \sigma_\epsilon^2 / n_B} \quad (11)$$

2.4 | Genotyping

Genotyping of the *M. sacchariflorus* diversity panel was performed using restriction site-associated DNA sequencing (RAD-seq). The RAD-seq library preparation was performed with the protocol described by Clark et al. (2014). In brief, genomic DNA from each genotype was digested with *Msp*I and

*Pst*I-HF restriction endonucleases (New England Biolabs) and ligated to barcoded *Pst*I and *Msp*I adaptors. The barcoded samples were pooled, size selected from 200 to 500 bp and amplified with a Kapa HiFi Library Amplification Kit (Kapa Biosystems, Wilmington, Massachusetts, USA). The resulting libraries were then sequenced on Illumina HiSeq 2500 and HiSeq 4000 instruments in the DNA Services Lab at the Roy J. Carver Biotechnology Center at the University of Illinois, using 100 nucleotide single-end reads beginning at the *Pst*I end of each fragment. The TASSEL-GBS pipeline (Bradbury et al. 2007) was used for read mapping and single-nucleotide polymorphism (SNP) calling against the *M. sinensis* v7.1 reference genome (DOE-JGI, http://phytozome.jgi.doe.gov/) (Mitros et al. 2020). SNPs obtained were imported into R and filtered to include only SNPs that had a minimum 70% call rate and a minor allele frequency of at least 0.05 in at least one of the six discriminant analysis of principal components (DAPC) groups previously identified by Clark et al. (2019). Genotype calling was performed using the population structure model in polyRAD version 1.6 (Clark, Lipka, and Sacks 2019). A total of 268,109 SNP markers were retained and used in subsequent GWAS.

2.5 | Genome-Wide Association Analyses

GWAS was performed using the Fixed and Random Model Circulating Probability Unification (FarmCPU) method described by Liu et al. (2016). The association analysis was performed on 205 *M. sacchariflorus* genotypes using 268,109 SNP markers, across 25 traits. We incorporated three principal components and a kinship matrix as covariates in the model to control for population structure and familial relatedness between genotypes. The Benjamini and Hochberg (1995) procedure was used to control the false discovery rate (FDR). SNPs with FDR-adjusted *p*-values of 0.05 were considered significant. We searched for candidate genes in the 10 kb region flanking the significant SNPs identified in the current study. A 10 kb region was chosen based on the low level of linkage disequilibrium in *Miscanthus* due to its outcrossing nature and undomesticated status (Slavov et al. 2014). We subsequently selected a subset of the most promising candidate genes based on whether the gene identified had functional annotation previously described in *Oryza sativa* or *Arabidopsis thaliana* consistent with it being causative for the trait in *M. sacchariflorus*.

3 | Results

3.1 | Variation in NPQ and ΦPSII Traits Across Treatments, Genetic Groups and Years

The change in NPQ or ΦPSII over time was used to deliver 25 traits describing NPQ and ΦPSII kinetics (Figure S2). For the majority of NPQ and ΦPSII traits, the general trend was for values from 2019 and 2020 being more similar to each other than to 2017 (Figure 1) as 2017 received less rainfall (216 cm) compared to 2019 (229 cm) and 2020 (275 cm) and had the highest average minimum (12.9°C) and average maximum (25.4°C) daily air temperature for the growing season (Figure S1). In all 3 years, median NPQ induction rates in light under chilling treatment were higher than those in the warm treatment (Figure 1a), indicating faster NPQ under chilling treatment. The median of NPQ induction in the light was on average 22%, 26% and 37% higher under chilling treatment compared to the corresponding warm treatment in 2017, 2019 and 2020, respectively. Most of the other NPQ traits pointed to the opposite trend, with higher values under warm than chilling treatment (Figure 1a,c,d,f). For instance, median of maximum level of NPQ assessed from the steady state of NPQ in light ($NPQasymptote_{lightH}$) was 7.4%, 13.3% and 12.9% lower in chilling than in the corresponding warm treatment in 2017, 2019 and 2020, respectively (Figure 1b). The not relaxed NPQ after 12 min of dark ($NPQresidual_{dark}$) among years in warm treatment ranged from 0.51 to 1.30, whereas in chilling ranged from 0.27 to 1.49 (Figure 1f). The rate of ΦPSII recovery in dark ($\Phi PSIIslope_{darkH}$) in the warm treatment was one of the most stable traits across the years with the median being 1.48, 1.49 and 1.51 in 2017, 2019 and 2020, respectively (Figure 1h). In response to chilling, the median of magnitude of ΦPSII change during 12 min of dark ($\Phi PSIIamplitute_{darkH}$) increased in all 3 years (Figure 3i). A similar trend was also observed for the level of ΦPSII recovery at the end of dark period ($\Phi PSII_{end}$) and ratio between ΦPSII recovered and NPQ not relaxed after 12 min of dark ($\Phi PSII_{end}/NPQ_{end}$) in 2017 and 2019 (Figure 1j,k).

Because 2020 had the most complete set of data (after quality control as described in the Material and Methods section), which could be attributed to it being the wettest year compared to other 2 years (Figure S1); we describe here in more detail NPQ and ΦPSII variation between genetic groups in that year. In the 2020 field season, greater variation was observed in NPQ and ΦPSII traits between genetic groups than within the genetic groups (Figures 2 and 3). Under the warm treatment, the NPQ induction rate in the light ($NPQslope_{lightH}$) ranged from 1.31 to 3.50 across 192 *M. sacchariflorus* genotypes (Figure 2a). The N China 2x group had the highest and the Yangtze 2x (ssp. *lutarioriparius*) group had the lowest median NPQ induction rates. Notably, under the chilling treatment, the median of NPQ induction rate increased for all genetic groups and the trait values ranged from 1.57 to 4.96. The highest increase in the median NPQ induction rate ($NPQslope_{lightH}$) under chilling relative to warm treatment was 83.9% in Yangtze 2x (ssp. *lutarioriparius*) followed by 58%, 42% and 39% for N Japan 4x, S Japan 4x and Korea/NE China/Russia 2x groups, respectively. Under chilling, the absolute value of median NPQ induction rate ($NPQslope_{lightH}$) was highest in the Korea/NE China/Russia 2x and N China 2x groups. Under the warm treatment, all genotypes from the Korea/NE China/Russia 2x and N China 2x groups had higher NPQ induction rates than the *M.* × *giganteus* '1993–1780' control, which is a commercially available accession with high chilling tolerance of photosynthesis and high yield (Figure 2a). However, under the chilling treatment, the median of NPQ induction rate of all the genetic groups was lower when compared to the *M.* × *giganteus* '1993–1780' control, which had a 1.75-fold increase of NPQ induction rate (Figure 2a).

When steady state of NPQ in light, assessed from the asymptote of hyperbolic fit to NPQ induction ($NPQasymptote_{lightH}$), was compared, the Yangtze 2x (ssp. *lutarioriparius*) group had the highest median steady state of NPQ (3.31) followed by the Korea/NE China/Russia 2x (3.18) and N China 2x (3.07) groups and the lowest value was observed for the S Japan 4x (2.78)

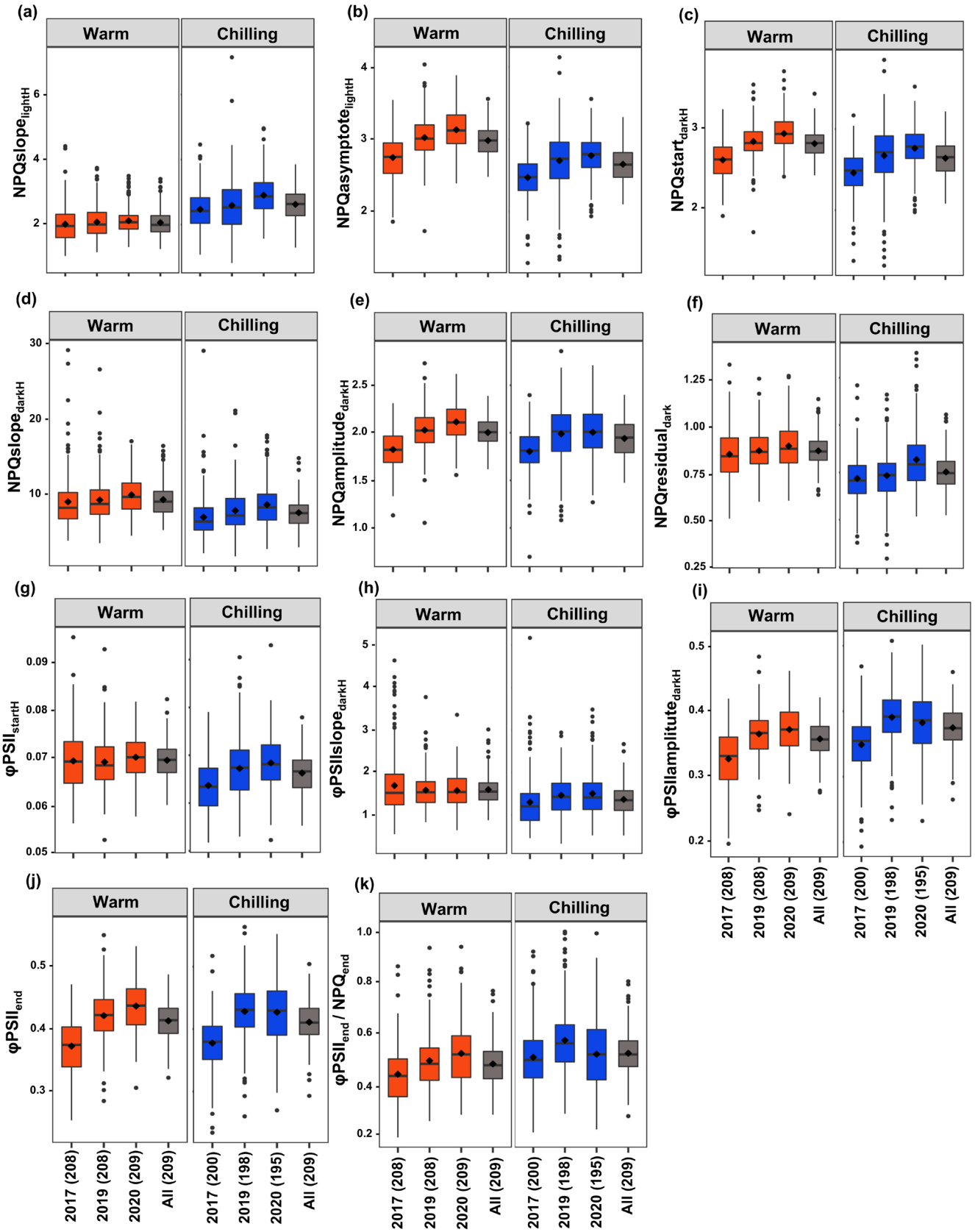

FIGURE 1 | Legend on next page.

group (Figure 2b), underlining different levels of photoprotection among groups. The median of steady state of NPQ in light was typically lower in chilling than warm treatment across all six *M. sacchariflorus* genetic groups, with the N China 2x and Korea/NE China/Russia 2x groups showing the smallest reduction (Figure 2b). Under chilling, the level of NPQ in the light

FIGURE 1 | Box plots showing variation in least square means for warm and chilling treatments in six NPQ and five φPSII traits for *Miscanthus sacchariflorus* diversity panel in three field seasons. Six traits describing induction of NPQ in light and relaxation in the dark are (a) rate of induction in light ($NPQslope_{lightH}$), (b) steady state in light ($NPQasymptote_{lightH}$), (c) NPQ at the beginning of the dark ($NPQstart_{darkH}$), (d) rate of relaxation in the dark ($NPQslope_{darkH}$), (e) magnitude of change in the dark ($NPQamplitude_{darkH}$) and (f) not relaxed NPQ at the end of the dark ($NPQresidual_{dark}$). Five traits describing recovery of φPSII in the dark are (g) φPSII at the beginning of dark ($\varphi PSII_{startH}$), (h) rate of recovery ($\varphi PSIIslope_{darkH}$), (i) magnitude of change ($\varphi PSIIamplitude_{darkH}$), (j) last point in the dark ($\varphi PSIIend$) and (k) ratio between φPSII recovered and NPQ not relaxed at the end of dark ($\varphi PSII_{end}/NPQ_{end}$). For a full description of the traits, see Table 1. The central box of the boxplot represents the interquartile range (25th–27th percentile in the data), the horizontal line within the box is median and the whiskers (upper and lower) represent data points that are above and below the interquartile range (1.5x interquartile range). The points beyond the whiskers are outliers. The number of genotypes studied in each year under warm or chilling treatment is indicated in parentheses below *x*-axis. Plants were grown in the afield trial at the University of Illinois Energy Farm located at 40.067 N, 88.198 W.

($NPQasymptote_{lightH}$) ranged from 1.93 to 3.56. When compared to the *M.* × *giganteus* '1993–1780' control under the warm treatment, all the genotypes of six *M. sacchariflorus* genetic groups had higher $NPQasymptote_{lightH}$. The same was true for N Japan 4x, Korea/NE China/Russia 2x and N China 2x groups under chilling treatment. Medians of $NPQasymptote_{lightH}$ for N China 2x and Korea/NE China/Russian 2x groups were 40% and 30% higher, respectively, than for the *M.* × *giganteus* '1993–1780' control.

Similar to the steady state of NPQ in the light, the NPQ at the start of dark ($NPQstart_{darkH}$), rate of NPQ relaxation in the dark ($NPQslope_{darkH}$) and magnitude of NPQ change during 12 min of dark ($NPQamplitude_{darkH}$) under the chilling treatment were reduced relative to the warm treatment in all but one of the genetic groups (Figure 2c–e). The exception was the N China 2x group, in which chilling resulted in marginal or moderate increases in the median of $NPQstart_{darkH}$ and $NPQamplitude_{darkH}$, respectively. $NPQslope_{darkH}$ ranged from 4.39 to 16.88 in warm, and from 2.69 to 17.71 under chilling. In the response to chilling, the median of not relaxed NPQ at the end of assay ($NPQresidual_{dark}$) increased in the N Japan 4x group, while staying the same or marginally lower in the rest of the genetic groups pointing to prolonged photoprotection under stress condition in the N Japan 4x group (Figure 2f). NPQ at the end of assay ($NPQresidual_{dark}$) ranged from 0.60 to 1.26 in warm and from 0.52 to 1.38 under chilling. Notably, the China 2x groups stood out for the highest residual NPQ at the end of dark. Under chilling, $NPQslope_{darkH}$ increased 1.25-fold in the *M.* × *giganteus* '1993–1780' control, whereas $NPQresidual_{dark}$ decreased 1.5-fold. As a consequence, under chilling, in all six *M. sacchariflorus* groups, the median of the NPQ relaxation rate was lower, and not relaxed NPQ after 12 min of dark was higher relative to the *M.* × *giganteus* '1993–1780' control (Figure 2d,f). These results suggest that all *M. sacchariflorus* groups under chilling conditions could have more sustainable NPQ than the *M.* × *giganteus* '1993–1780' control, leading to higher chilling tolerance.

The ΦPSII at the start of the dark was only marginally different between treatments and genotypes (Figure 3a). The rate of ΦPSII recovery in dark ($\Phi PSIIslope_{darkH}$) ranged from 0.64 to 3.36 in warm and from 0.51 to 3.49 under chilling (Figure 3b). In response to chilling, the $\Phi PSIIslope_{darkH}$ median did not change or changed marginally in the N China/Korea/Russia 4x and Korea/NE China/Russia 2x groups, respectively, whereas the other genetic groups had a 14% to 32.8% reduction. However, the genotypes with the highest $\Phi PSIIslope_{darkH}$ under warm and chilling treatments belonged to the Korea/NE China/Russia 4x group. In response to chilling, the Korea/NE China/Russia 4x and N China 2x groups displayed increased or maintained similar median values for magnitude of ΦPSII response in dark ($\Phi PSIIamplitute_{darkH}$), $\Phi PSII_{end}$ and estimation of tradeoff between the quantum efficiency of photochemistry and NPQ ($\Phi PSII_{end}/NPQ_{end}$) (Figure 3c–e), suggesting higher efficiency of light reaction of photosynthesis in these genetic groups under chilling stress. In contrast, the other *M. sacchariflorus* genetic groups exhibited a reduction of the same traits reaching up to −75% in the median of $\Phi PSII_{end}/NPQ_{end}$ for the N Japan 4x group. Under chilling, in comparison to the *M.* × *giganteus* '1993–1780' control, all *M. sacchariflorus* genotypes had lower values for five ΦPSII traits. Interestingly, triploid *M.* × *giganteus* 'Nagara', under both warm and chilling conditions, had higher values of $\Phi PSIIamplitute_{darkH}$ and $\Phi PSII_{end}$ than the *M.* × *giganteus* '1993–1780' control (Figure 3c,d). Similar variations in NPQ and ΦPSII traits were observed in the other two growing seasons, 2017 and 2019 (Figures S3–S6).

Pairwise trait correlations showed that the rate of NPQ induction in warm and chilling was only negligible correlated with a maximum value of NPQ (e.g., on average −0.04 for $NPQslope_{light\ H}$ and $NPQasymptote_{lightH}$; Figures S7 and S8). In contrast, the rates estimated for instance from the exponential equation of NPQ relaxation and ΦPSII recovery were highly positively correlated (≥0.90) both in warm and chilling. Although the chilling treatment slightly changed correlation values between traits, the direction of correlation remained the same with no clear trend in making the correlation stronger or weaker. As different equations in addition to single-measured timepoints were used to estimate the same attributes of NPQ and ΦPSII kinetics, it might not be surprising that different traits describing the same portion of the curves showed highly positive correlations regardless of the treatment, for example, NPQ_{end} and $NPQresidual_{dark}$ (0.98); NPQ_{max}, $NPQasymptote_{lightE}$ and $NPQasymptote_{lightH}$ (on average 0.98); and $\Phi PSIIamplitude_{darkH}$ and $\Phi PSIIamplitude_{darkE}$ (0.99).

The average broad-sense heritability for all 25 NPQ and ΦPSII traits studied was 0.58, 0.42 and 0.46 in 2017, 2019 and 2020, respectively (Table S2). In 2017, broad-sense heritability ranged from 0.48 (ΦPSII at the beginning of the dark) to 0.69 ($NPQslope_{lightH}$). The average heritability of traits for all years together was lower than the average heritability of individual years, thus leading us to choose 2 years (2017 and 2020) with the highest heritability for identification of candidate genes using

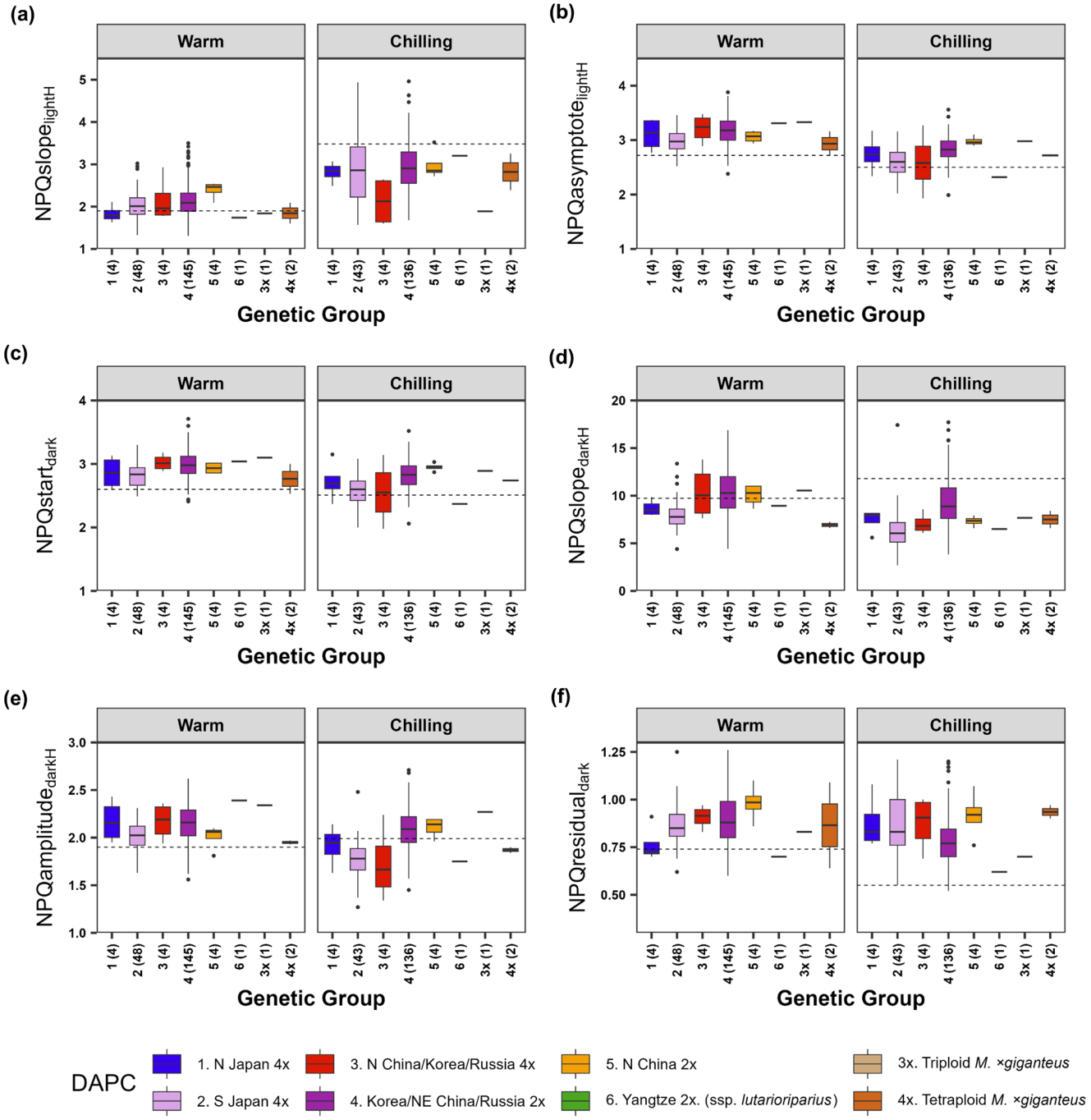

FIGURE 2 | Box plots showing variation in genotype least square means for warm and chilling treatments in NPQ traits among six genetic groups of *Miscanthus sacchariflorus* and two ploidy groups of *M.* × *giganteus* in the 2020 field season. Six traits describing induction of NPQ in light and relaxation in the dark are (a) rate of induction in light ($NPQslope_{lightH}$), (b) steady state in light ($NPQasymptote_{lightH}$), (c) NPQ at the beginning of the dark ($NPQstart_{darkH}$), (d) rate of relaxation in the dark ($NPQslope_{darkH}$), (e) magnitude of change in the dark ($NPQamplitude_{darkH}$) and (f) not relaxed NPQ at the end of the dark ($NPQresidual_{dark}$). For a full description of the traits, see Table 1. The colours represent the genetic groups of *M. sacchariflorus* and ploidy groupings of *M.* × *giganteus*. The genetic groups of *M. sacchariflorus* were previously identified by discriminant analysis of principal components (Clark et al. 2019). The number of genotypes studied in each group/ploidy is indicated in parentheses on the *x*-axis. The horizontal dashed line represents the value for the *M.* × *giganteus* 3x '1993–1780' (it was not included in the boxplot for *M.* × *giganteus* 3x because it serves as control due to being the most studied *Miscanthus* accession and known for its high chilling tolerance). The central box of the boxplot represents the interquartile range (25th–27th percentile in the data), the horizontal line within the box is median and the whiskers (upper and lower) represent data points that are above and below the interquartile range (1.5x interquartile range). The points beyond the whiskers are outliers. Plants were grown in the afield trial at the University of Illinois Energy Farm located at 40.067 N, 88.198 W.

GWAS. The average heritability of traits for chilling to warm ratio was low (0.34); thus, it was not used for the GWAS study.

3.2 | Identification of Genomic Regions and Candidate Genes Involved in NPQ and ΦPSII Kinetics

Using the data from 2 years with the highest average broad-sense heritability, a total of 126 significant SNP marker—trait associations were identified across six *M. sacchariflorus* genetic groups at the significance level $p < 0.05$. Out of 126 SNPs, there were 90 highly significant SNPs ($p < 0.01$; Table S3). A total of 21 SNPs were significant for more than one trait. The trait combinations that shared significant SNPs were NPQ in the last point in the dark (NPQ_{end}) and not relaxed NPQ at the end in the dark ($NPQresidual_{dark}$); ΦPSII in the last point in the dark ($\Phi PSII_{end}$) and range of ΦPSII response in the dark expressed as $\Phi PSIIamplitude_{darkH}$ and $\Phi PSIIamplitude_{darkE}$; highest value of NPQ induction (NPQ_{max}) and NPQ at the beginning of dark ($NPQstart_{darkH}$); rate of the NPQ induction in the light expressed as $NPQslope_{lightL}$ and $NPQslope_{lightH}$ and steady-state NPQ expressed as $NPQasymptote_{lightH}$ and $NPQasymptote_{lightE}$. A total of 99 significant SNPs were found to be within a 10 kb window of a gene. For 83 candidate genes, *A. thaliana* (Arabidopsis) and/or *O. sativa* (rice) orthologs were identified. The analysis by the genomic region showed that 16.7% ($n = 21$) of the significant SNPs were in exon regions of the *M. sinensis* reference genome. However, the rest of the significant SNPs were in the non-coding regions, which includes 27.8% ($n = 35$) in intergenic regions, 19% ($n = 24$) in upstream regions, 16.7% ($n = 21$) in downstream regions, 10.3% ($n = 13$) in introns and 9.6% ($n = 12$) in untranslated regions (3′ and 5′ UTR; Figure 4). We highlighted seven promising candidate genes, near SNPs that had highly significant associations with photosynthetic traits (Table 2; Figure 5). These promising candidate genes include two homeologs of Hydroxycinnamoyl-CoA Shikimate/Quinate Hydroxycinnamoyl Transferase (*HCT*), monodehydroascorbate Reductase 1 (*MDAR1*), high-affinity gamma-aminobutyric acid (GABA) transporter (*GAT1*), pentatricopeptide repeat (*PPR*) superfamily protein, MYB-domain protein 105 (*MYB105*) and a cation efflux family protein.

4 | Discussion

Substantial variation for traits describing distinct attributes of photoprotection and efficiency of the light reaction of photosynthesis was observed among and within the genetic groups of *M. sacchariflorus* under warm and chilling conditions (Figures 2 and 3; Figures S3–S6). This indicates that existing natural variation in *M. sacchariflorus* might be sufficient for the breeding of new *M.* × *giganteus* cultivars with high photoprotection from excess light under chilling and high efficiency of light reaction under warm conditions. Similar to the previous study on the *M. sacchariflorus* diversity panel for yield-component traits (Njuguna, Clark, Anzoua et al. 2023), we found that variation among genetic groups for physiological traits was typically greater than the variation within those groups. This suggests that the genetic group should be a key consideration when making crosses to breed new *M.* × *giganteus* cultivars.

Notably, the northernly adapted Korea/NE China/Russia 2x and N China 2x groups stood out under the chilling treatment for having one of the highest increases in the NPQ rate in light in combination with the highest retention of steady state NPQ in the light (Figure 2a,b). For example, accession RU2012-112, which belongs to the Korea/NE China/Russia 2x group, was identified in this study as having 18% faster induction of NPQ under chilling compared to *M.* × *giganteus*; moreover, Pignon et al. (2019) previously reported that this accession retained 7% more assimilation capacity after 15 days of growth under chilling temperatures (5/10°C night/day).

Fast induction of NPQ in the dark would be expected to contribute better protection of photosystem II from oxidative stress, particularly during bright and chilling mornings that commonly occur in spring and autumn in temperate environments. This observation might be explained by enhanced accumulation of zeaxanthin under chilling because it is a pigment crucial for the qZ portion of NPQ (Bethmann et al. 2019). A higher level of zeaxanthin after a chilling night in the Korea/NE China/Russia 2x and N China 2x genotypes could be due to de novo synthesis of zeaxanthin in response to chilling or its faster conversion from violaxanthin and antheraxanthin by upregulation of VDE (Haupt and Głowacka 2024). Another possibility is the retention of zeaxanthin over the chilling night via downregulation of ZEP, which converts zeaxanthin back to violaxanthin. Interestingly, light-independent accumulation of zeaxanthin was observed in other photosynthesizing organisms that are adapted to extremely challenging environments, for example, during the winter for evergreen trees (Adams and Demmig-Adams 1994; Brüggemann et al. 2009) and in response to desiccation and freezing for subalpine herbaceous resurrection plants (Fernández-Marín et al. 2018). A previous screening of 51 *Miscanthus* genotypes also identified an accession from the Korea/NE China/Russia 2x group that retained leaf growth under chilling conditions equivalent to *M.* × *giganteus* '1993–1780' (Głowacka et al. 2014).

Additionally, in response to chilling in the current study, the Korea/NE China/Russia 2x and N China 2x groups exhibited increased or maintained similar values of the amplitude of ΦPSII induction in the dark, ΦPSII at the end of 12 min induction in the dark and the ratio between induced ΦPSII and not relax NPQ after 12 min of the dark (Figure 3c–e), indicating that they maintained photosynthetic efficiency under chilling conditions. This suggests that the Korea/NE China/Russia 2x and N China 2x groups might be good resources for identifying genotypes with both high photoprotection from excess light ($NPQslope_{lightH}$, $NPQasymptote_{lightH}$) and maintaining high efficiency of the light reaction under chilling stress ($\Phi PSIIamplitude_{darkH}$, $\Phi PSII_{end}$ and $\Phi PSII_{end}/NPQ_{end}$). Pignon et al. (2019) similarly identified three *M. sacchariflorus* accessions from the Korea/NE China/Russia 2x group with superior chilling tolerance of photosynthesis relative to *M.* × *giganteus* '1993–1780'.

We also observed that one accession of the Yangtze 2x (ssp. *lutarioriparius*) group, which was previously observed to have outstanding biomass production (Njuguna, Clark, Anzoua et al. 2023), had the highest recovery of ΦPSII in the dark and the highest tradeoff between the quantum efficiency of photochemistry and NPQ ($\Phi PSII_{end}$ / NPQ_{end}) under warm treatment, suggesting superior efficiency of the light reaction of

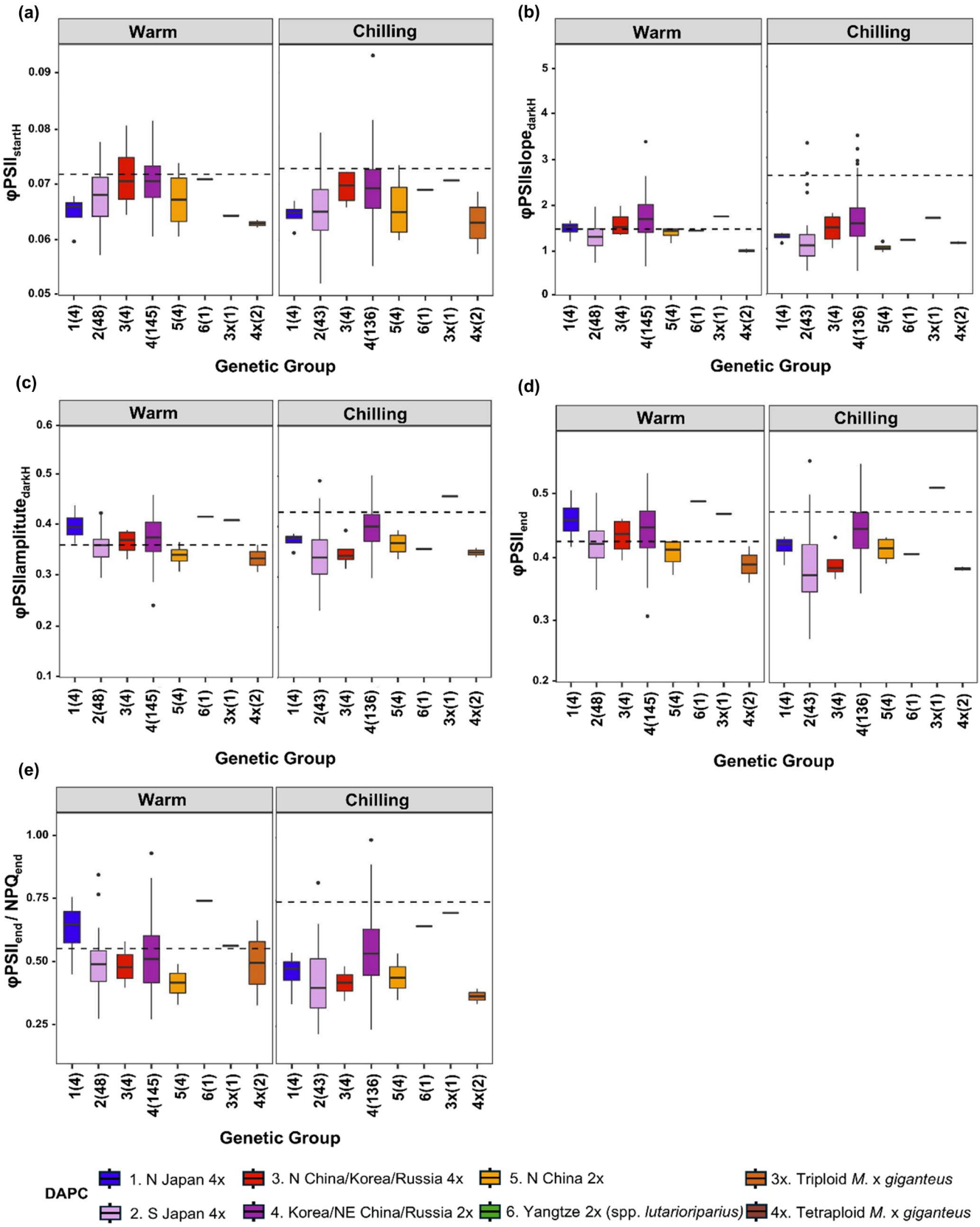

FIGURE 3 | Legend on next page.

photosynthesis (Figure 3 c, e). Both of these traits were substantially higher in this Yangtze 2x (ssp. *lutarioriparius*) accession than in the *M.* × *giganteus* '1993–1780' control (12.2% and 36.3%, respectively), suggesting that they may contribute to the former's high productivity. However, under the chilling treatment, the subtropical-adapted Yangtze 2x (ssp. *lutarioriparius*) accession had the lowest steady-state level of NPQ, which likely contributed to the low chilling tolerance of this accession (Figure 2b).

FIGURE 3 | Box plots showing variation in genotype least square means for warm and chilling treatments in φPSII traits among six genetic groups of *Miscanthus sacchariflorus* and two ploidy groups of *M.* × *giganteus* in the 2020 field season. Five traits describing recovery of φPSII in the dark are (a) φPSII at the beginning of dark ($\varphi PSII_{startH}$), (b) rate of recovery ($\varphi PSIIslope_{darkH}$), (c) magnitude of change ($\varphi PSIIamplitude_{darkH}$), (d) last point in the dark ($\varphi PSIIend$) and (e) ratio between φPSII recovered and NPQ not relaxed at the end of dark ($\varphi PSII_{end}/NPQ_{end}$). For a full description of the traits, see Table 1. The colours represent the genetic groups of *M. sacchariflorus* and ploidy groupings *M.* × *giganteus*. The genetic groups of *M. sacchariflorus* were previously identified by discriminant analysis of principal components (Clark et al. 2019). The number of genotypes studied in each group/ploidy is indicated in parentheses below the *x*-axis. The horizontal dashed line represents the value for the *M.* × *giganteus* 3x '1993–1780' (it was not included in the boxplot for *M.* × *giganteus* 3x because it serves as control due to being the most studied *Miscanthus* accession and known for its high chilling tolerance). The central box of the boxplot represents the interquartile range (25th–27th percentile in the data), the horizontal line within the box is median and the whiskers (upper and lower) represent data points that are above and below the interquartile range (1.5x interquartile range). The points beyond the whiskers are outliers. Plants were grown in the afield trial at the University of Illinois Energy Farm located at 40.067 N, 88.198 W.

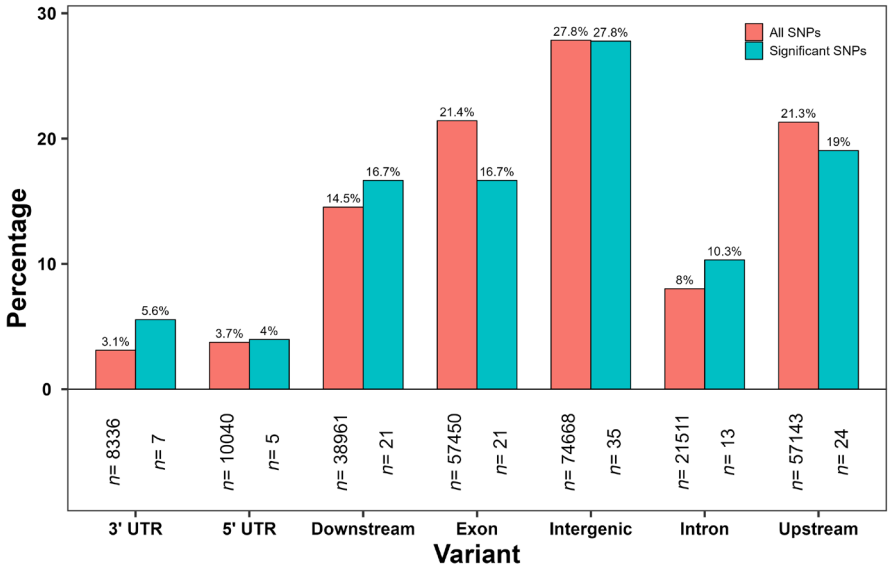

FIGURE 4 | Bar plot showing gene regions for 126 significant single-nucleotide polymorphisms (SNPs) identified compared to gene regions of all 268,109 SNPs used in the genome-wide association study of 25 NPQ and ΦPSII traits in 205 *Miscanthus sacchariflorus* genotypes.

Here, we identified 126 unique SNPs associated with one or more photosynthesis traits (Table S3). Using a similar semi-high-throughput method for NPQ and ΦPSII phenotyping, Sahay et al. (2023) identified a comparable number of SNPs associated with variation in NPQ and/or ΦPSII kinetics in a maize diversity panel grown under field conditions. In *Sorghum bicolor*, a GWAS for only the single trait of ΦPSII under control conditions resulted in the identification of 12 SNPs (Ortiz, Hu, and Salas Fernandez 2017). Two QTLs associated with the high NPQ induction were identified in *O. sativa* (Kasajima et al. 2011). The greater number of SNPs identified in our study compared to the previous work in sorghum or rice may be due to our approach of dissecting of NPQ and ΦPSII kinetics into several component traits to explain different attributes of kinetics, rate, steady state and range of change, or by differences in the statistical approaches employed for GWAS, or simply by inherent differences among the species and populations in the different studies.

We highlighted seven promising candidate genes near SNPs that had highly significant associations ($p < 0.01$) with photosynthesis traits (Table 2; Figure 5). The candidate gene that was mechanistically the most closely related to NPQ and ΦPSII regulation and associated with ΦPSII at the beginning of the dark in chilling was Misin04G127400.1 (Figure 5a), an ortholog of Arabidopsis *MDAR1* (Table 2; Figure 5a). The crucial enzyme for NPQ induction, VDE, needs for its activity an ascorbate cofactor, which is converted to monodehydroascorbate by enzymatic reaction and then recycled back to ascorbate with the help of MDAR. MDAR is important for maintaining a pool of reduced ascorbate via ascorbate regeneration, and the ascorbate concentration closely correlates with NPQ (Chen and Gallie 2008; Müller-Moulé, Conklin, and Niyogi 2002). The SNP located in the 3'UTR of *MDAR1* (Table S4) was associated with ΦPSII at the beginning of the dark in chilling. Since quenching via photochemical processes (ΦPSII) and NPQ compete for energy, the ΦPSII at the beginning of dark has a strong negative relationship with the steady state of NPQ in the light. Lack of ascorbate in *Arabidopsis* ascorbate-deficient mutant (*vtc2*) resulted in a lower NPQ rate compared to the wild type but the NPQ rate could be restored by feeding detached leaves of exogenous ascorbate (Müller-Moulé, Conklin, and Niyogi 2002). In contrast, overexpression of *MDAR* was reported to enhance tolerance of photosynthesis to multiple abiotic stresses in transgenic tobacco (Eltayeb et al. 2007). MDAR can also indirectly affect NPQ via the Mehler-peroxidase reaction, which maintains the electron flow to PSI from PSII without evolution of net oxygen.

TABLE 2 | Summary for seven selected candidate genes that were near SNPs that had highly significant photosynthesis trait associations in *Miscanthus sacchariflorus*.

Miscanthus sinensis gene	Gene description	*Arabidopsis thaliana* ortholog	*Zea mays* ortholog	Chromosome	Position	Trait	Treatment	Year
Misin02G231300.1	Hydroxycinnamoyl-CoA shikimate/quinate hydroxycinnamoyl transferase	AT5G48930	ZmPHB47.01G224600.1	2	61,531,179	$NPQslope_{darkH}$	Warm	2017
Misin19G197700.1	Hydroxycinnamoyl-CoA shikimate/quinate hydroxycinnamoyl transferase	AT5G48930	Zm00001d039833_T001	19	68,622,013	$\Phi PSII_{end} / NPQ_{end}$	Chilling	2020
Misin04G127400.1	Monodehydroascorbate reductase 1	AT3G52880	Zm00001d005347_T001	4	38,660,047	$\Phi PSII_{startH}$	Chilling	2017
Misin03G345000.1	Pentatricopeptide repeat (PPR) superfamily protein	AT1G26900	ZmPHB47.K123000.1	3	105,426,542	$\Phi PSII_{end} / NPQ_{end}$	Warm	2017
Misin07G303200.1	MYB domain protein 105	AT1G69560	ZmPHB47.01G332900.1	7	72,909,843	$\Phi PSII_{end} / NPQ_{end}$	Chilling	2020
Misin11G033100.1	Cation efflux family protein	AT1G51610	Zm00008a007698_T01	11	21,067,592	$\Phi PSII_{end} / NPQ_{end}$	Chilling	2020
Misin05G332100.1	Transmembrane amino acid transporter family protein (GAT1)	AT1G08230	ZmPHJ40.K061900.1	5	100,443,368	$NPQresidual_{dark}$	Chilling	2020

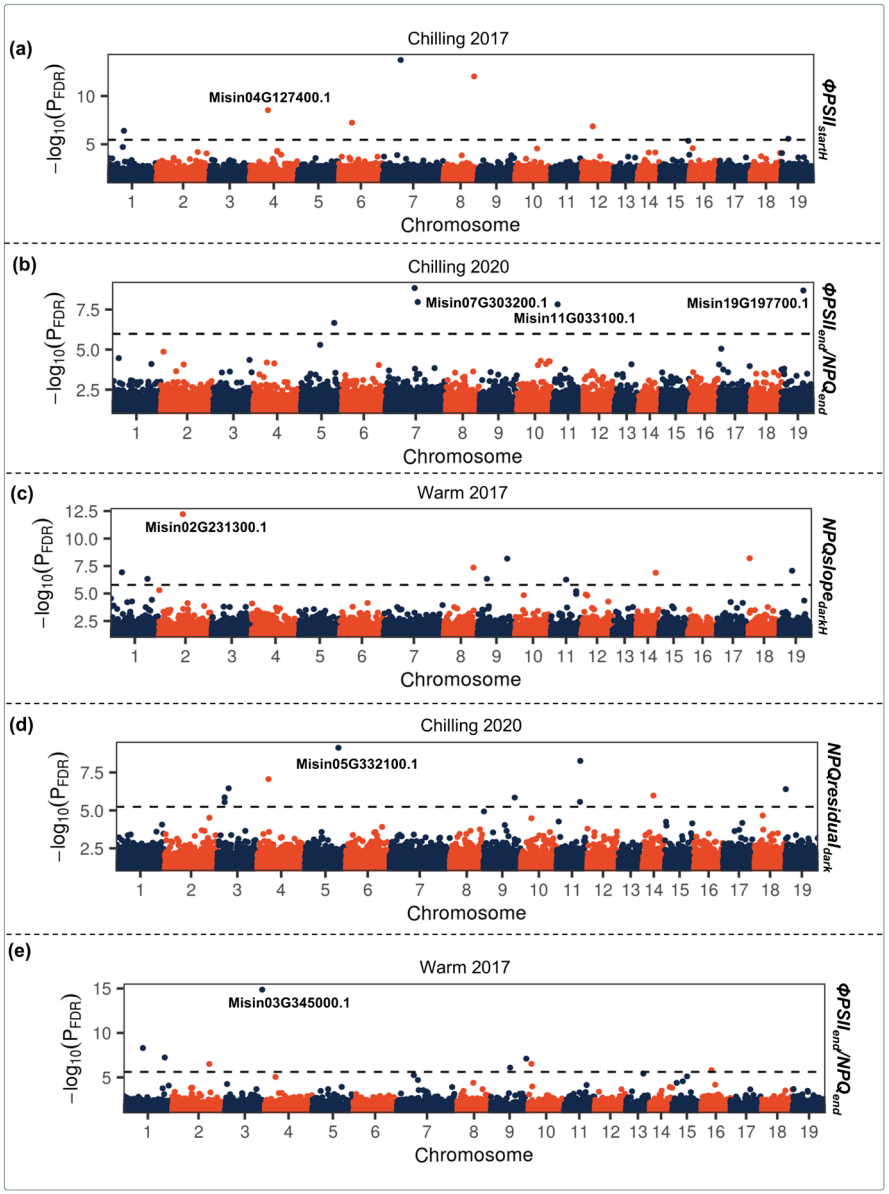

FIGURE 5 | Results of genome-wide association studies (GWAS) conducted on four traits calculated from the NPQ and ΦPSII curves for a *Miscanthus sacchariflorus* diversity panel under warm (2017) or chilling (2017 and 2020) treatments. (a) ΦPSII at the beginning of the dark ($\Phi PSII_{startH}$) for chilling treatment in 2017, (b) $\Phi PSII_{end}/\ NPQ_{end}$ for chilling treatment in 2020, (c) rate of NPQ relaxation in the dark ($NPQslope_{darkH}$) for warm treatment in 2017, (d) not relax NPQ at the end of the dark ($NPQresidual_{dark}$) for chilling treatment in 2020 and (e) ratio between ΦPSII recovered and NPQ not relaxed at the end of dark ($\Phi PSII_{end}/\ NPQ_{end}$) for warm treatment in 2017. The *x*-axis indicates the position of SNPs on the reference genome of *Miscanthus sinensis* v7.1. The *y*-axis indicates log-transformed FDR-corrected *p*-values. The dashed line indicates the significance threshold at FDR-adjusted *p*-values = 0.0.

This pseudo-cyclic electron flow was shown to generate a proton gradient important for energy-dependent quenching and zeaxanthin formation in the intact chloroplast of *Lactuca sativa* L. (lettuce) under the condition of limited CO_2 fixation (Neubauer and Yamamoto 1992). Interestingly, the candidate gene, Misin15G055400.1, an ortholog of Arabidopsis L-galactono-1,4-lactone dehydrogenase (*GLDH*), a gene that catalyzes the final step of ascorbate biosynthesis, was also significantly associated with the rate of NPQ induction in light.

Two homeologs of *HCT*, Misin02G231300.1 on chromosome 2 and Misin19G197700.1 on chromosome 19, were identified near significant SNPs. *HCT* was the only candidate gene, which we identified by two SNPs, both positioned in the upstream region of the gene, and each significantly associated with different traits: NPQ slope in the dark (warm treatment 2017) and the ratio of ΦPSII and NPQ at the endpoint in the dark (chilling treatment 2020) (Table 2; Figure 5b,c). HCT utilises the intermediates of the shikimate pathway for the production of lignin through the phenylpropanoid pathway, playing a decisive role for the channeling of shikimate pathway intermediates (Cabane, Afif, and Hawkins 2012). Therefore, the downregulation of *HCT* would channel more intermediates of the shikimate pathway towards the production of aromatic amino acids that are upstream substrates for flavonoid and anthocyanin syntheses (Yuan et al. 2022). Interestingly, an increase in anthocyanins was reported for a

highly chilling tolerant *Miscanthus* accession relative to a low chilling tolerant one (Haupt and Głowacka 2024). Anthocyanins act as light attenuators, working in synergy with NPQ for photoprotection (Zhu et al. 2018). Thus, HCT appears to have an indirect role in regulating NPQ under warm and chilling conditions. Interestingly, low temperature stimulates phenylpropanoid and shikimate pathways (Cabane, Afif, and Hawkins 2012; Zhou et al. 2019). For instance, in winter, *Hordeum vulgare* L. (barley) exposed to cold stress showed upregulation of *HCT* after acclimatisation at −3°C (Janská et al. 2011).

Two other SNPs associated with the same trait, tradeoff between the quantum efficiency of photochemistry and NPQ ($\Phi PSII_{end}/NPQ_{end}$), which estimates the tradeoff between ΦPSII recovered and NPQ not relaxed after 12 min of dark in chilling treatment (a low ratio indicates dark quenching of excess energy via NPQ that serves as a protective mechanism for the photosystem under chilling stress), were located on chromosomes 7 and 11 in the introns of Misin07G303200.1 and Misin11G033100.1, respectively (Figure 5b). The gene Misin07G303200.1 was identified as an Arabidopsis ortholog of a *MYB105*. The MYB transcription factor plays an important role in plant response to abiotic stresses, including chilling and freezing tolerance (Vannini et al. 2004). The gene Misin11G033100.1 was identified as an Arabidopsis ortholog of chloroplast-located cation efflux family protein and is reported to be an ion antiporter. One cation/proton antiporter protein, K^+ efflux antiporter (KEA3), has been demonstrated to accelerate the energy-dependent (qE) component of NPQ and therefore contribute to maintaining photosynthetic efficiency under fluctuating light conditions (Armbruster et al. 2014).

The SNP most strongly associated with residual NPQ in the dark under chilling treatment was located downstream of gene Misin05G332100.1 on chromosome 5 (Figure 5d), which is a *Miscanthus* ortholog of an Arabidopsis gene that encodes for an H^+-driven, high-affinity GAT1. Elevated concentration of GABA was reported to increase chilling tolerance and cold tolerance in tomato, barley, wheat, banana and *Camellia sinensis* (L. Li et al. 2021; Malekzadeh, Khara, and Heydari 2014; Mazzucotelli et al. 2006; Wang et al. 2014; Zhu et al. 2019).

The most significant SNP ($p < 0.001$) we observed originated from a synonymous SNP residing within an exon of the Misin03G345000.1 gene on chromosome 3, identified as an ortholog of Arabidopsis *PPR* superfamily protein (Figure 5e). The PPR proteins perform post-transcriptional regulation of organelle genes, such as those in chloroplasts and mitochondria (Barkan and Small, 2014) and in principle could indirectly effect ΦPSII or/and NPQ via regulation of genes encoding the photosynthetic apparatus. This SNP was associated with the ratio of the dark end-points of ΦPSII and NPQ ($\Phi PSII_{end}/NPQ_{end}$) in the warm treatment.

Here, we demonstrated that semi-high-throughput imaging of leaf disc fluorescence in 96-well plates can be successfully deployed to screen a germplasm panel for NPQ and ΦPSII under chilling treatment. Modification of this approach opens the possibility to study kinetics of NPQ and ΦPSII in a semi-high-throughput way under gradients of temperatures in combination with a variety of incubation times. Notably, our results indicated that after chilling treatment, all *M. sacchariflorus* genetic groups increased the NPQ induction rate. Under chilling, the Korea/NE China/Russia 2x and N China 2x groups stood out for the highest NPQ rate in light and the highest steady-state NPQ in light. That was also true for residual NPQ at the end of dark for the N China 2x group. In addition, some genetic groups also exhibited an increase in residual NPQ after 12 min of dark incubation. Both of these phenotypes likely contribute to adaptation to chilling during sunny mornings that follow chilling nights, where faster and more sustainable NPQ would protect from oxidative stress. Among the detected candidate genes related to the regulation of NPQ and ΦPSII kinetics, especially promising is *MDAR1*, which is involved in recycling the ascorbate, a cofactor for a key enzyme (VDE) involved in the qZ component of NPQ. By identifying natural variation and genes involved in NPQ and ΦPSII kinetics, we considerably expand the toolbox for breeding and/or engineering *Miscanthus* and other Saccharinae to have optimised photosynthesis under warm and chilling conditions for sustainable and high biomass production.

Author Contributions

Asha Kumari: data curation, formal analysis, visualization, writing – original draft, writing – review and editing. **Joyce N. Njuguna:** data curation, formal analysis, investigation, methodology, visualization, writing – review and editing. **Xuying Zheng:** investigation, writing – review and editing. **Johannes Kromdijk:** conceptualization, investigation, writing – review and editing. **Erik J. Sacks:** funding acquisition, resources, supervision, visualization, writing – review and editing. **Katarzyna Glowacka:** conceptualization, funding acquisition, methodology, project administration, supervision, visualization, writing – original draft, writing – review and editing.

Acknowledgments

The authors thank Jared Haupt and Evan LaBran for assistance with field data collection. They also thank the field team at the Energy Farm of the University of Illinois who helped to establish and maintain the field trial.

Conflicts of Interest

The authors declare no conflicts of interest.

Data Availability Statement

The data that support the findings of this study are openly available in Figshare at https://doi.org/10.6084/m9.figshare.27948354.v1.

References

Adams, W. W., and B. Demmig-Adams. 1994. "Carotenoid Composition and Down Regulation of Photosystem II in Three Conifer Species During the Winter." *Physiologia Plantarum* 92, no. 3: 451–458. https://doi.org/10.1111/J.1399-3054.1994.TB08835.X.

Armbruster, U., L. R. Carrillo, K. Venema, et al. 2014. "Ion Antiport Accelerates Photosynthetic Acclimation in Fluctuating Light Environments." *Nature Communications* 5, no. 1. https://doi.org/10.1038/ncomms6439.

Barkan, A., and I. Small. 2014. "Pentatricopeptide Repeat Proteins in Plants." *Annual Review of Plant Biology* 65, no. 1: 415–442. https://doi.org/10.1146/annurev-arplant-050213-040159.

Bates, D., M. Mächler, B. M. Bolker, and S. C. Walker. 2015. "Fitting Linear Mixed-Effects Models Using lme4." *Journal of Statistical Software* 67, no. 1: 1–48. https://doi.org/10.18637/jss.v067.i01.

Benjamini, Y., and Y. Hochberg. 1995. "Controlling the False Discovery Rate: A Practical and Powerful Approach to Multiple Testing." *Journal of the Royal Statistical Society: Series B: Methodological* 57, no. 1: 289–300. https://doi.org/10.1111/J.2517-6161.1995.TB02031.X.

Bethmann, S., M. Melzer, N. Schwarz, and P. Jahns. 2019. "The Zeaxanthin Epoxidase Is Degraded Along With the D1 Protein During Photoinhibition of Photosystem II." *Plant Direct* 3, no. 11: e00185. https://doi.org/10.1002/PLD3.185.

Bradbury, P. J., Z. Zhang, D. E. Kroon, T. M. Casstevens, Y. Ramdoss, and E. S. Buckler. 2007. "TASSEL: Software for Association Mapping of Complex Traits in Diverse Samples." *Bioinformatics* 23, no. 19: 2633–2635. https://doi.org/10.1093/BIOINFORMATICS/BTM308.

Brüggemann, W., M. Bergmann, K. U. Nierbauer, E. Pflug, C. Schmidt, and D. Weber. 2009. "Photosynthesis Studies on European Evergreen and Deciduous Oaks Grown Under Central European Climate Conditions: II. Photoinhibitory and Light-Independent Violaxanthin Deepoxidation and Downregulation of Photosystem II in Evergreen, Winter-Acclimated European Quercus Taxa." *Trees-Structure and Function* 23, no. 5: 1091–1100. https://doi.org/10.1007/S00468-009-0351-Y/FIG.S/8.

Cabane, M., D. Afif, and S. Hawkins. 2012. "Lignins and Abiotic Stresses." In *Advances in Botanical Research*, vol. 61, 1st ed. Academic Press, USA: Elsevier Ltd. https://doi.org/10.1016/B978-0-12-416023-1.00007-0.

Chen, Z., and D. R. Gallie. 2008. "Dehydroascorbate Reductase Affects Non-photochemical Quenching and Photosynthetic Performance." *Journal of Biological Chemistry* 283, no. 31: 21347–21361. https://doi.org/10.1074/jbc.M802601200.

Chiluwal, A., R. Bheemanahalli, R. Perumal, et al. 2018. "Integrated Aerial and Destructive Phenotyping Differentiates Chilling Stress Tolerance During Early Seedling Growth in Sorghum." *Field Crops Research* 227: 1–10. https://doi.org/10.1016/J.FCR.2018.07.011.

Clark, L. V., J. E. Brummer, K. Głowacka, et al. 2014. "A Footprint of Past Climate Change on the Diversity and Population Structure of *Miscanthus sinensis*." *Annals of Botany* 114, no. 1: 97–107. https://doi.org/10.1093/AOB/MCU084.

Clark, L. V., X. Jin, K. K. Petersen, et al. 2019. "Population Structure of *Miscanthus sacchariflorus*Reveals Two Major Polyploidization Events, Tetraploid-Mediated Unidirectional Introgression From Diploid *M. Sinensis*, and Diversity Centred Around the Yellow Sea." *Annals of Botany* 124, no. 4: 731–748. https://doi.org/10.1093/AOB/MCY161.

Clark, L. V., A. E. Lipka, and E. J. Sacks. 2019. "polyRAD: Genotype Calling With Uncertainty From Sequencing Data in Polyploids and Diploids." *G3: Genes, Genomes, Genetics* 9, no. 3: 663–673. https://doi.org/10.1534/G3.118.200913.

Clifton-Brown, J., Y. C. Chiang, and T. R. Hodkinson. 2008. "Miscanthus: Genetic Resources and Breeding Potential to Enhance Bioenergy Production." In *Genetic Improvement of Bioenergy Crops*, edited by W. Vermerris, vol. 3, 161–182. New York, NY: Springer. https://doi.org/10.1007/978-0-387-70805.

Clifton-Brown, J., A. Harfouche, M. D. Casler, et al. 2019. "Breeding Progress and Preparedness for Mass-Scale Deployment of Perennial Lignocellulosic Biomass Crops Switchgrass, Miscanthus, Willow and Poplar." *GCB Bioenergy* 11, no. 1: 118–151. https://doi.org/10.1111/gcbb.12566.

Clifton-Brown, J., K. U. Schwarz, D. Awty-Carroll, et al. 2019. "Breeding Strategies to Improve Miscanthus as a Sustainable Source of Biomass for Bioenergy and Biorenewable Products." *Agronomy* 9, no. 11: 673. https://doi.org/10.3390/AGRONOMY9110673.

Cousins, A. B., N. R. Adam, G. W. Wall, et al. 2002. "Photosystem II Energy Use, Non-photochemical Quenching and the Xanthophyll Cycle in *Sorghum bicolor* Grown Under Drought and Free-Air CO_2Enrichment (FACE) Conditions." *Plant, Cell and Environment* 25, no. 11: 1551–1559. https://doi.org/10.1046/j.1365-3040.2002.00935.x.

Dall'Osto, L., S. Caffarri, and R. Bassi. 2005. "A Mechanism of Nonphotochemical Energy Dissipation, Independent From PsbS, Revealed by a Conformational Change in the Antenna Protein CP26." *Plant Cell* 17, no. 4: 1217–1232. https://doi.org/10.1105/TPC.104.030601.

Demmig-Adams, B. 1990. "Carotenoids and Photoprotection in Plants: A Role for the Xanthophyll Zeaxanthin." *Biochimica et Biophysica Acta (BBA)—Bioenergetics* 1020, no. 1: 1–24. https://doi.org/10.1016/0005-2728(90)90088-L.

Deuter, M. 2009. "Miscanthus Plant Named 'MBS 7001' U.S. Patent No. US PP22,033 P2."

Dong, H., S. Liu, L. V. Clark, et al. 2019. "Winter Hardiness of Miscanthus (II): Genetic Mapping for Overwintering Ability and Adaptation Traits in Three Interconnected Miscanthus Populations." *GCB Bioenergy* 11, no. 5: 706–726. https://doi.org/10.1111/gcbb.12587.

Eltayeb, A. E., N. Kawano, G. H. Badawi, et al. 2007. "Overexpression of Monodehydroascorbate Reductase in Transgenic Tobacco Confers Enhanced Tolerance to Ozone, Salt and Polyethylene Glycol Stresses." *Planta* 225, no. 5: 1255–1264. https://doi.org/10.1007/s00425-006-0417-7.

Fernández-Marín, B., G. Neuner, E. Kuprian, J. M. Laza, J. I. García-Plazaola, and A. Verhoeven. 2018. "First Evidence of Freezing Tolerance in a Resurrection Plant: Insights Into Molecular Mobility and Zeaxanthin Synthesis in the Dark." *Physiologia Plantarum* 163, no. 4: 472–489. https://doi.org/10.1111/ppl.12694.

Friesen, P. C., M. M. Peixoto, F. A. Busch, D. C. Johnson, and R. F. Sage. 2014. "Chilling and Frost Tolerance in Miscanthus and Saccharum Genotypes Bred for Cool Temperate Climates." *Journal of Experimental Botany* 65, no. 13: 3749–3758. https://doi.org/10.1093/jxb/eru105.

Głowacka, K., S. Adhikari, J. Peng, et al. 2014. "Variation in Chilling Tolerance for Photosynthesis and Leaf Extension Growth Among Genotypes Related to the C_4Grass *Miscanthus* × *Giganteus*." *Journal of Experimental Botany* 65, no. 18: 5267–5278. https://doi.org/10.1093/jxb/eru287.

Głowacka, K., L. V. Clark, S. Adhikari, et al. 2015. "Genetic Variation in *Miscanthus* × *Giganteus* and the Importance of Estimating Genetic Distance Thresholds for Differentiating Clones." *GCB Bioenergy* 7, no. 2: 386–404. https://doi.org/10.1111/GCBB.12166.

Haupt, J., and K. Głowacka. 2024. "Chilling- and Dark-Regulated Photoprotection in *Miscanthus*, an Economically Important C_4Grass." *Communications Biology* 7: 1660. https://doi.org/10.1038/s42003-024-07320-0.

Hodkinson, T., and S. Renvoize0. 2001. "Nomenclature of *Miscanthus* × *Giganteus* (Poaceae)." *Kew Bulletin* 56: 759–760.

Janská, A., A. Aprile, J. Zámečník, L. Cattivelli, and J. Ovesná. 2011. "Transcriptional Responses of Winter Barley to Cold Indicate Nucleosome Remodelling as a Specific Feature of Crown Tissues." *Functional and Integrative Genomics* 11, no. 2: 307–325. https://doi.org/10.1007/s10142-011-0213-8.

Kafadar, K., J. R. Koehler, W. N. Venables, and B. D. Ripley. 2002. "Modern Applied Statistics With S Fourth Edition." *Journal of the Royal Statistical Society* 51, no. 2: 86. https://doi.org/10.2307/2685660.

Kalinina, O., C. Nunn, R. Sanderson, et al. 2017. "Extending Miscanthus Cultivation With Novel Germplasm at Six Contrasting Sites." *Frontiers in Plant Science* 8: 254524. https://doi.org/10.3389/FPLS.2017.00563/BIBTEX.

Kasajima, I., K. Ebana, T. Yamamoto, et al. 2011. "Molecular Distinction in Genetic Regulation of Nonphotochemical Quenching in Rice." *Proceedings of the National Academy of Sciences of the United States of America* 108, no. 33: 13835–13840. https://doi.org/10.1073/pnas.1104809108.

Kromdijk, J., K. Głowacka, L. Leonelli, et al. 2016. "Improving Photosynthesis and Crop Productivity by Accelerating Recovery From Photoprotection." *Science* 354, no. 6314: 857–862.v.

Kumari, A. 2024. "Dataset 1: Genetic basis of non-photochemical quenching and photosystem II efficiency responses to chilling in the biomass crop *Miscanthus*." https://doi.org/10.6084/m9.figshare.27948354.v1.

Langholtz, M. H., B. J. Stokes, and L. M. Eaton. 2016. "Billion-Ton Report: Advancing Domestic Resources for a Thriving Bioeconomy." In *Volume 1: Economic Availability of Feedstocks. U.S. Department of Energy*. Oak Ridge, TN: Oak Ridge National Laboratory. https://doi.org/10.2172/1271651.

Lee, D. K., E. Aberle, E. K. Anderson, et al. 2018. "Biomass Production of Herbaceous Energy Crops in the United States: Field Trial Results and Yield Potential Maps From the Multiyear Regional Feedstock Partnership." *GCB Bioenergy* 10, no. 10: 698–716. https://doi.org/10.1111/GCBB.12493.

Leipner, J., Y. Fracheboud, and P. Stamp. 1999. "Effect of Growing Season on the Photosynthetic Apparatus and Leaf Antioxidative Defenses in Two Maize Genotypes of Different Chilling Tolerance." *Environmental and Experimental Botany* 42, no. 2: 129–139. https://doi.org/10.1016/S0098-8472(99)00026-X.

Lenth, R. V. 2016. "Least-Squares Means: The R Package Lsmeans." *Journal of Statistical Software* 69: 1–33. https://doi.org/10.18637/JSS.V069.I01.

Li, L., N. Dou, H. Zhang, and C. Wu. 2021. "The Versatile GABA in Plants." *Plant Signaling & Behavior* 16, no. 3: e1862565. https://doi.org/10.1080/15592324.2020.1862565.

Li, X. P., O. Björkman, C. Shih, et al. 2000. "A Pigment-Binding Protein Essential for Regulation of Photosynthetic Light Harvesting." *Nature* 403, no. 6768: 391–395. https://doi.org/10.1038/35000131.

Linde-Laursen, I. 1993. "Cytogenetic Analysis of Miscanthus 'Giganteus', an Interspecific Hybrid." *Hereditas* 119, no. 3: 297–300. https://doi.org/10.1111/J.1601-5223.1993.00297.X.

Liu, X., M. Huang, B. Fan, E. S. Buckler, and Z. Zhang. 2016. "Iterative Usage of Fixed and Random Effect Models for Powerful and Efficient Genome-Wide Association Studies." *PLoS Genetics* 12, no. 2: e1005767. https://doi.org/10.1371/JOURNAL.PGEN.1005767.

Ma, Y., X. Dai, Y. Xu, et al. 2015. "COLD1 Confers Chilling Tolerance in Rice." *Cell* 160, no. 6: 1209–1221. https://doi.org/10.1016/j.cell.2015.01.046.

Malekzadeh, P., J. Khara, and R. Heydari. 2014. "Alleviating Effects of Exogenous Gamma-Aminobutiric Acid on Tomato Seedling Under Chilling Stress." *Physiology and Molecular Biology of Plants* 20, no. 1: 133–137. https://doi.org/10.1007/S12298-013-0203-5/FIG.S/1.

Malnoë, A. 2018. "Photoinhibition or Photoprotection of Photosynthesis? Update on the (Newly Termed) Sustained Quenching Component qH." *Environmental and Experimental Botany* 154: 123–133. https://doi.org/10.1016/J.ENVEXPBOT.2018.05.005.

Mazzucotelli, E., A. Tartari, L. Cattivelli, and G. Forlani. 2006. "Metabolism of γ-Aminobutyric Acid During Cold Acclimation and Freezing and Its Relationship to Frost Tolerance in Barley and Wheat." *Journal of Experimental Botany* 57, no. 14: 3755–3766. https://doi.org/10.1093/JXB/ERL141.

Mitros, T., A. M. Session, B. T. James, et al. 2020. "Genome Biology of the Paleotetraploid Perennial Biomass Crop Miscanthus." *Nature Communications* 11, no. 5442: 1–11. https://doi.org/10.1038/s41467-020-18923-6.

Müller, P., X. P. Li, and K. K. Niyogi. 2001. "Non-Photochemical Quenching. A Response to Excess Light Energy." *Plant Physiology* 125, no. 4: 1558–1566. https://doi.org/10.1104/PP.125.4.1558.

Müller-Moulé, P., P. L. Conklin, and K. K. Niyogi. 2002. "Ascorbate Deficiency Can Limit Violaxanthin de-Epoxidase Activity In Vivo." *Plant Physiology* 128, no. 3: 970–977. https://doi.org/10.1104/pp.010924.

Naidu, S. L., S. P. Moose, A. K. Al-shoaibi, C. A. Raines, and S. P. Long. 2003. "Cold Tolerance of C_4Photosynthesis in *Miscanthus* × *Giganteus*: Adaptation in Amounts and Sequence of C_4Photosynthetic Enzymes." *Plant Physiology* 132: 1688–1697. https://doi.org/10.1104/pp.103.021790.photosynthetic.

Neubauer, C., and H. Y. Yamamoto. 1992. "Mehler-Peroxidase Reaction Mediates Zeaxanthin Formation and Zeaxanthin-Related Fluorescence Quenching in Intact Chloroplasts." *Plant Physiology* 99, no. 4: 1354–1361. https://doi.org/10.1104/pp.99.4.1354.

Nilkens, M., E. Kress, P. Lambrev, et al. 2010. "Identification of a Slowly Inducible Zeaxanthin-Dependent Component of Non-photochemical Quenching of Chlorophyll Fluorescence Generated Under Steady-State Conditions in Arabidopsis." *Biochimica et Biophysica Acta (BBA) - Bioenergetics* 1797, no. 4: 466–475. https://doi.org/10.1016/J.BBABIO.2010.01.001.

Njuguna, J. N., L. V. Clark, K. G. Anzoua, et al. 2023. "Biomass Yield in a Genetically Diverse *Miscanthus sacchariflorus*Germplasm Panel Phenotyped at Five Locations in Asia, North America, and Europe." *GCB Bioenergy* 15, no. 5: 642–662. https://doi.org/10.1111/gcbb.13043.

Njuguna, J. N., L. V. Clark, A. E. Lipka, et al. 2023. "Genome-Wide Association and Genomic Prediction for Yield and Component Traits of *Miscanthus sacchariflorus*." *GCB Bioenergy* 15, no. 11: 1355–1372. https://doi.org/10.1111/gcbb.13097.

Ortiz, D., J. Hu, and M. G. Salas Fernandez. 2017. "Genetic Architecture of Photosynthesis in *Sorghum bicolor* Under Non-stress and Cold Stress Conditions." *Journal of Experimental Botany* 68, no. 16: 4545–4557. https://doi.org/10.1093/JXB/ERX276.

Pignon, C. P., I. Spitz, E. J. Sacks, U. Jørgensen, K. Kørup, and S. P. Long. 2019. "Siberian *Miscanthus sacchariflorus*Accessions Surpass the Exceptional Chilling Tolerance of the Most Widely Cultivated Clone of *Miscanthus* × *Giganteus*." *GCB Bioenergy* 11, no. 7: 883–894. https://doi.org/10.1111/gcbb.12599.

Rapacz, M., M. Tyrka, W. Kaczmarek, M. Gut, B. Wolanin, and W. Mikulski. 2008. "Photosynthetic Acclimation to Cold as a Potential Physiological Marker of Winter Barley Freezing Tolerance Assessed Under Variable Winter Environment." *Journal of Agronomy and Crop Science* 194, no. 1: 61–71. https://doi.org/10.1111/J.1439-037X.2007.00292.X.

Roach, T., and A. Krieger-Liszkay. 2012. "The Role of the PsbS Protein in the Protection of Photosystems I and II Against High Light in *Arabidopsis thaliana*." *Biochimica et Biophysica Acta (BBA)—Bioenergetics* 1817, no. 12: 2158–2165. https://doi.org/10.1016/J.BBABIO.2012.09.011.

Sacks, E. J., J. A. Juvik, Q. J. Lin, R. J. Stewart, and T. Yamada. 2013. "The Gene Pool of Miscanthus Species and Its Improvement." In *Genomics of the Saccharinae. Plant Genetics and Genomics: Crops and Models*, edited by A. Paterson, vol. 11. New York, NY: Springer. https://doi.org/10.1007/978-1-4419-5947-8.

Sahay, S., M. Grzybowski, J. C. Schnable, and K. Głowacka. 2023. "Genetic Control of Photoprotection and Photosystem II Operating Efficiency in Plants." *New Phytologist* 239, no. 3: 1068–1082. https://doi.org/10.1111/NPH.18980.

Savitch, L. V., E. D. Leonardos, M. Krol, et al. 2002. "Two Different Strategies for Light Utilization in Photosynthesis in Relation to Growth and Cold Acclimation." *Plant, Cell and Environment* 25, no. 6: 761–771. https://doi.org/10.1046/j.1365-3040.2002.00861.x.

Slavov, G. T., R. Nipper, P. Robson, et al. 2014. "Genome-Wide Association Studies and Prediction of 17 Traits Related to Phenology, Biomass and Cell Wall Composition in the Energy Grass *Miscanthus sinensis*." *New Phytologist* 201, no. 4: 1227–1239. https://doi.org/10.1111/NPH.12621.

Somerville, C., H. Youngs, C. Taylor, S. C. Davis, and S. P. Long. 2010. "Feedstocks for Lignocellulosic Biofuels." *Science* 329, no. 5993: 790–792. https://doi.org/10.1126/SCIENCE.1189268/SUPPL_FILE/SOMERVILLE-SOM.PDF.

Vannini, C., F. Locatelli, M. Bracale, et al. 2004. "Overexpression of the Rice *Osmyb4*Gene Increases Chilling and Freezing Tolerance of *Arabidopsis thaliana* Plants." *Plant Journal* 37, no. 1: 115–127. https://doi.org/10.1046/J.1365-313X.2003.01938.X.

Wang, D., A. R. Portis, S. P. Moose, and S. P. Long. 2008. "Cool C_4Photosynthesis: Pyruvate P_iDikinase Expression and Activity Corresponds to the Exceptional Cold Tolerance of Carbon Assimilation in *Miscanthus* × *Giganteus*." *Plant Physiology* 148, no. 1: 557–567. https://doi.org/10.1104/pp.108.120709.

Wang, Y., Z. Luo, X. Huang, K. Yang, S. Gao, and R. Du. 2014. "Effect of Exogenous γ-Aminobutyric Acid (GABA) Treatment on Chilling Injury and Antioxidant Capacity in Banana Peel." *Scientia Horticulturae* 168: 132–137. https://doi.org/10.1016/J.SCIENTA.2014.01.022.

Yamamoto, H. Y., T. O. M. Nakayama, and C. O. Chichester. 1962. "Studies on the Light and Dark Interconversions of Leaf Xanthophylls." *Archives of Biochemistry and Biophysics* 97, no. 1: 168–173. https://doi.org/10.1016/0003-9861(62)90060-7.

Yuan, J., S. Zhong, Y. Long, J. Guo, Y. Yu, and J. Liu. 2022. "Shikimate Kinase Plays Important Roles in Anthocyanin Synthesis in Petunia." *International Journal of Molecular Sciences* 23, no. 24: 1–15. https://doi.org/10.3390/ijms232415964.

Zhou, P., Q. Li, G. Liu, et al. 2019. "Integrated Analysis of Transcriptomic and Metabolomic Data Reveals Critical Metabolic Pathways Involved in Polyphenol Biosynthesis in *Nicotiana tabacum*Under Chilling Stress." *Functional Plant Biology* 46, no. 1: 30–43. https://doi.org/10.1071/FP18099.

Zhu, H., T. J. Zhang, J. Zheng, et al. 2018. "Anthocyanins Function as a Light Attenuator to Compensate for Insufficient Photoprotection Mediated by Nonphotochemical Quenching in Young Leaves of *Acmena Acuminatissima* in Winter." *Photosynthetica* 56, no. 1: 445–454. https://doi.org/10.1007/s11099-017-0740-1.

Zhu, X., J. Liao, X. Xia, et al. 2019. "Physiological and iTRAQ-Based Proteomic Analyses Reveal the Function of Exogenous γ-Aminobutyric Acid (GABA) in Improving Tea Plant (*Camellia sinensis* L.) Tolerance at Cold Temperature." *BMC Plant Biology* 19, no. 1: 1–20. https://doi.org/10.1186/S12870-019-1646-9/FIG.S/11.

Supporting Information

Additional supporting information can be found online in the Supporting Information section.